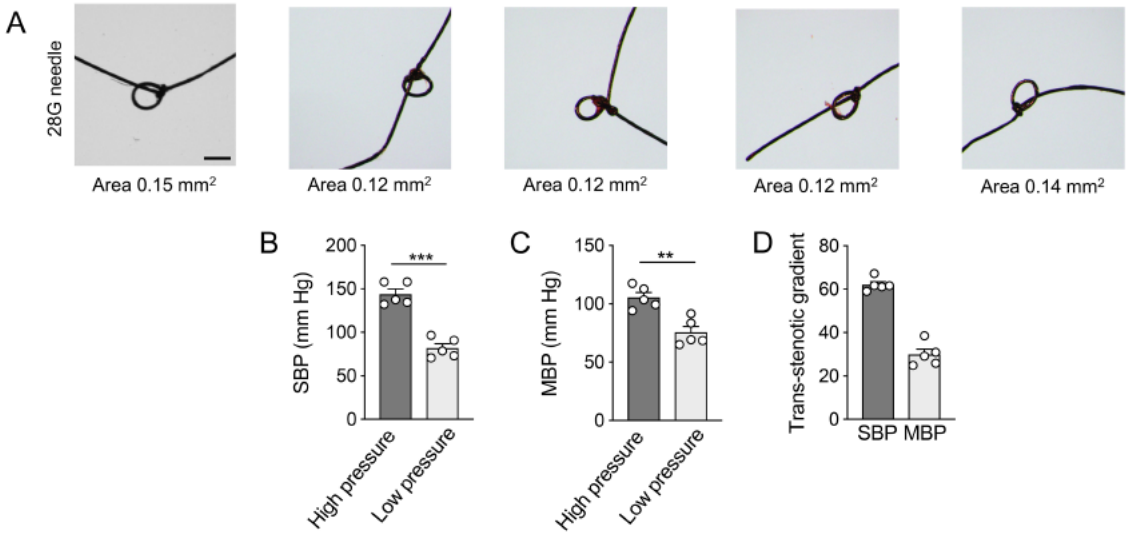

Supplemental Figure 1. Trans-stenotic gradient in TAC-operated ApoE$^{-/-}$ mice. ApoE$^{-/-}$ mice have been subjected to TAC surgery using a 28-gauge needle. (A) Images of suture ligature around the 28-gauge needle performed in ApoE$^{-/-}$ mice. The area of each ligature placed around the aortic arch is reported from five mice. The following day, the trans-stenotic gradient has been measured by by using radiotelemetry device. A catheter (HD-X10) was inserted through the right and then left carotid artery to measure the trans-stenotic pressure gradient. (B) Systolic blood pressure (SBP) and (C) mean blood pressure (MBP) were measured upstream (high pressure) and downstream (low pressure) the aortic banding. (D) Trans-stenotic gradient expressed as difference in SBP and MBP, upstream and downstream the banding. **, P<0.01; ***, P<0.001, unpaired t-test (n=5). Scale bars: 500 μm.

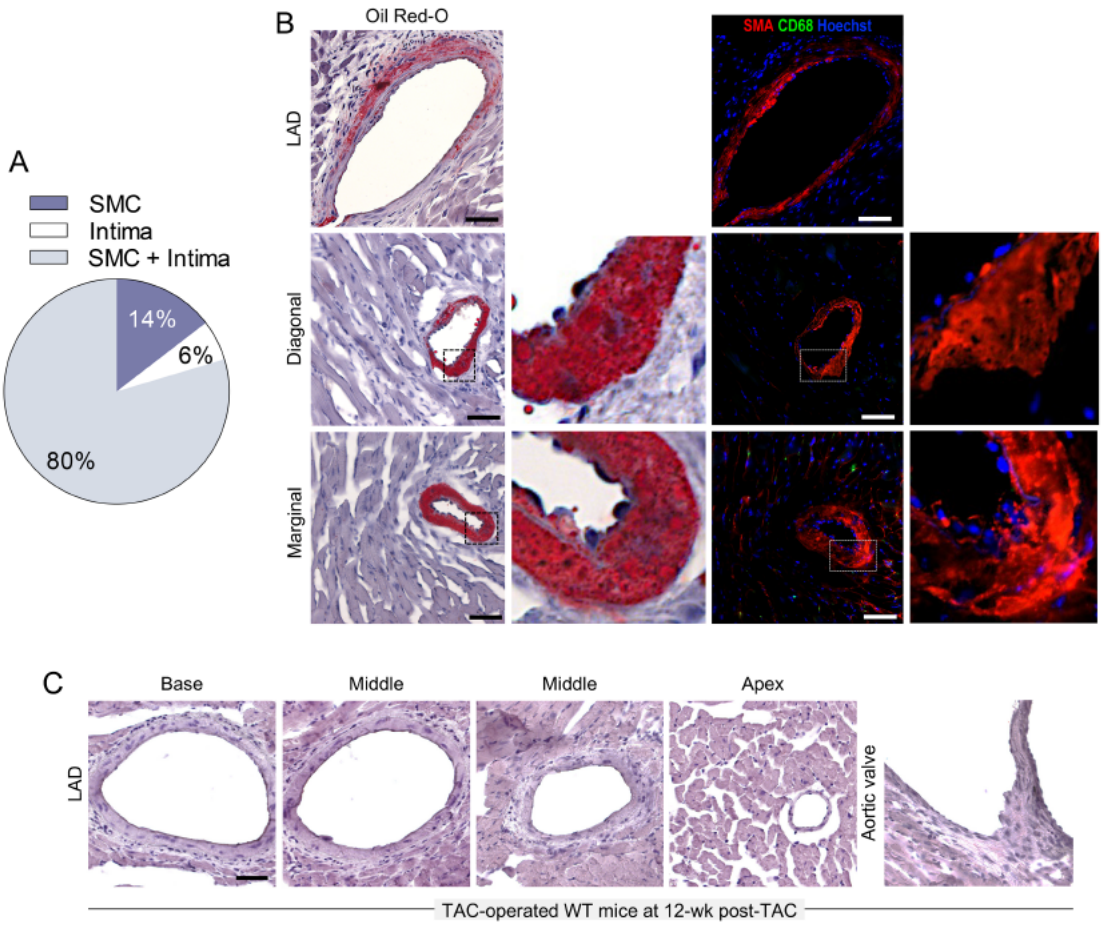

Supplemental Figure 2. Lipid deposition in coronary early lesions of ApoE$^{-/-}$ mice at 8-week post-TAC and WT mice at 12-wk post-TAC. (A) Pie chart representing the distribution of lipids accumulation into the coronary wall: in 80% of early lesions lipids accumulate in both SMC and intima; in 14% of the early lesions lipids accumulate in SMC; and in 6% of the cases in the intima (n=103 coronary lesions from 10 mice). (B) Myocardial sections of ApoE$^{-/-}$ mouse at 8-week post-TAC were stained with oil red-O & hematoxylin, and immunofluorescently stained with α-SMA (SMC), CD68 (monocyte/macrophage) and Hoechst (nuclei). Oil red-O showed lipid accumulation in the media of proximal LAD, and diagonal and marginal arteries. Immunofluorescent staining for α-SMA (red) confirms the accumulation of lipids into smooth muscle cells, while co-staining for CD68 is negative. Nuclei were stained with Hoechst (blue). (C) Myocardial sections of WT (C57BL/6) mice at 12-week post-TAC, stained with oil red-O & hematoxylin, did not show any evidence of coronary lesions. Scale bars: 50 μm.

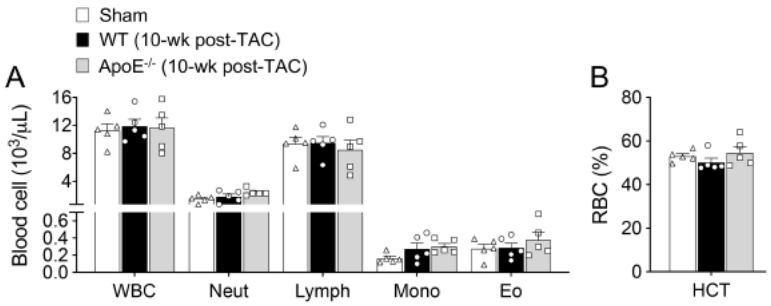

Supplemental Figure 3. Blood cell count at 10 weeks TAC-operated WT and ApoE$^{-/-}$ mice, and sham-operated ApoE$^{-/-}$ mice. (A) White blood cell (WBC) and (B) red blood cells (RBC) counts in sham-operated ApoE$^{-/-}$ mice and TAC-operated WT and ApoE$^{-/-}$ mice 10 weeks after TAC. At this time point no differences were observed in the overall blood population (n>5). Neut, neutrophils; Lymph, lymphocytes; Mono, monocytes; Eo, eosinophils; HCT, hematocrit.

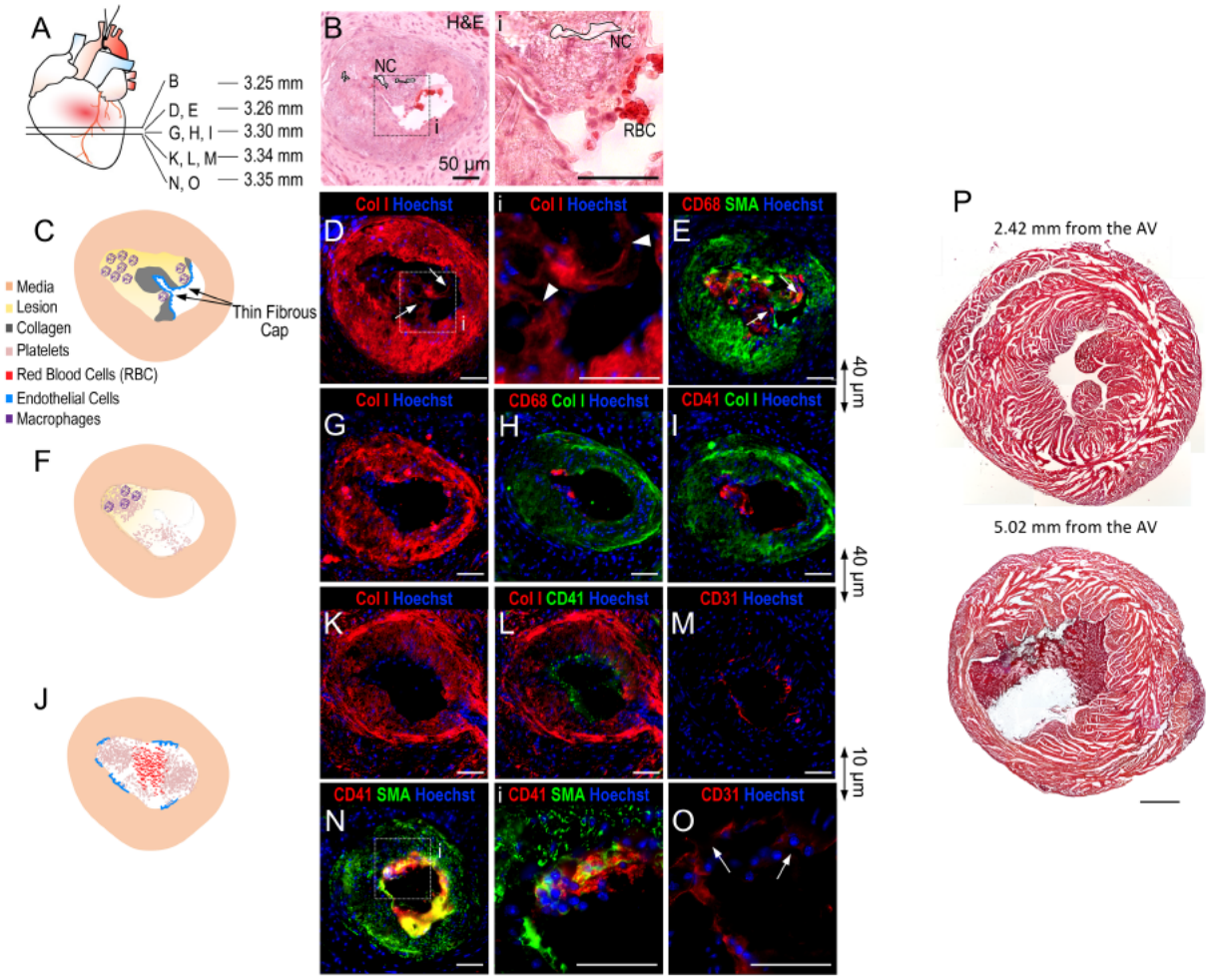

Supplemental Figure 4. Coronary plaque rupture and thrombotic occlusion in ApoE$^{-/-}$ mice post-TAC. (A) Scheme of the localization of immunofluorescently labeled heart sections proximal and distal to the section with thrombus shown in panel B and inset i. NC=necrotic core. (B) At 3.25 mm from the AV there is a major lesion as shown by the H&E staining and inset i. (D,E) IF staining showed a very thin fibrous cap (Col I and α-SMA staining) in two points (panel D, inset i, arrowheads). (E) IF staining for CD68 shows macrophage accumulation in close proximity to the thin fibrous cap (arrows). (C) Schematic representation of the plaque in the LAD based on panels D,E. (G-I) IF staining of consecutive myocardial sections for Col I (red), macrophages (CD68, red), platelets (CD41, red) and smooth muscle cells (α-SMA, green) reveal that the major part of plaque detached from the coronary wall. In panel H is still possible to notice some remaining CD68 positive cells of the lipid core of the plaque, and in panel I platelets aggregates interacting with CD68-positive cells and ruptured plaque. (F) Schematic representation of the IF staining in panels G-I. (K-O) Consecutive downstream sections showing platelet aggregates in intimate contact with the plaque downstream the point of rupture. (O) It is possible to observe the disruption of the endothelial layer, possibly by erosion, and platelets aggregates in correspondence of the disrupted endothelium in contact with SMC (panel N, inset i). (J) Schematic cartoon representing the IF staining in panels K-O of the thrombotic event in the LAD. Scale bars: 50 µm. (P) Masson's trichrome staining of the medium and apex of the heart at the indicated distance from the AV.

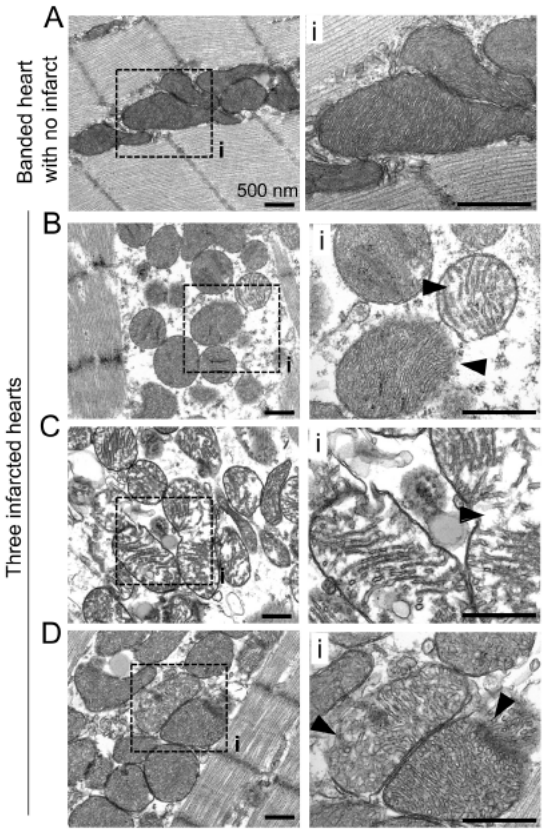

Supplemental Figure 5. Mitochondria morphology and cristae architecture in the infarcted hearts of ApoE$^{-/-}$ mice post-TAC. (A) Representative transmission electron micrographs of cardiac mitochondria of control mice (ApoE$^{-/-}$ without evidence of MI, and C57BL/6 at the same time post-TAC). (B-D) Representative images of mitochondria from infarcted hearts of three ApoE$^{-/-}$ mice with swollen mitochondria and disorganization of cristae (B and C, arrowheads), loss of mitochondrial double membrane (D, arrowheads). Scale bars: 500 nm.

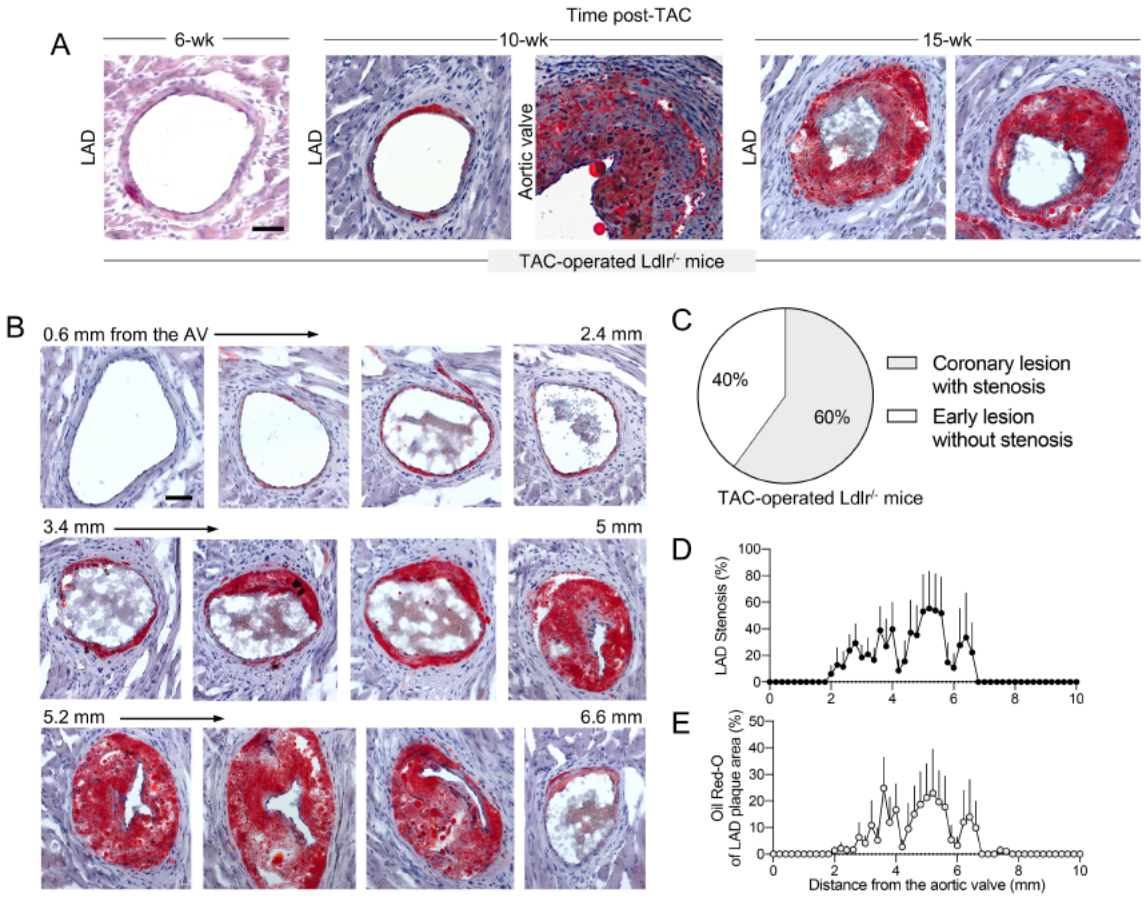

Supplemental Figure 6. Characterization and distribution of coronary lesions in chow-fed Ldlr$^{-/-}$ mice post-TAC. (A) At 6-wk, 10-wk and 15-wk post-TAC, sequential myocardial sections of Ldlr$^{-/-}$ mice were stained with oil red-O & hematoxylin. At 6-wk and 10-wk post-TAC Ldlr$^{-/-}$ mice presented only early lesions in the coronary arteries. Specifically, lipid accumulation was detected in the intima, media or both, without any protrusion into the lumen. At 15 weeks post-TAC, Ldlr$^{-/-}$ mice developed coronary lesion with stenosis. (B) Oil red-O & hematoxylin staining of myocardial sections showing the LAD of a chow-fed Ldlr$^{-/-}$ mouse. (C) The pie chart shows the percentage of Ldlr$^{-/-}$ mice with early lesions with no stenosis, and coronary lesions with stenosis (n=5). (D) Quantification of LAD stenosis from the AV to the apex of 15-wk TAC-operated Ldlr$^{-/-}$ mice (n=3). (E) Base-to-apex lipid accumulation into the same LAD lesions, expressed as percentage of the plaque area (n=3).

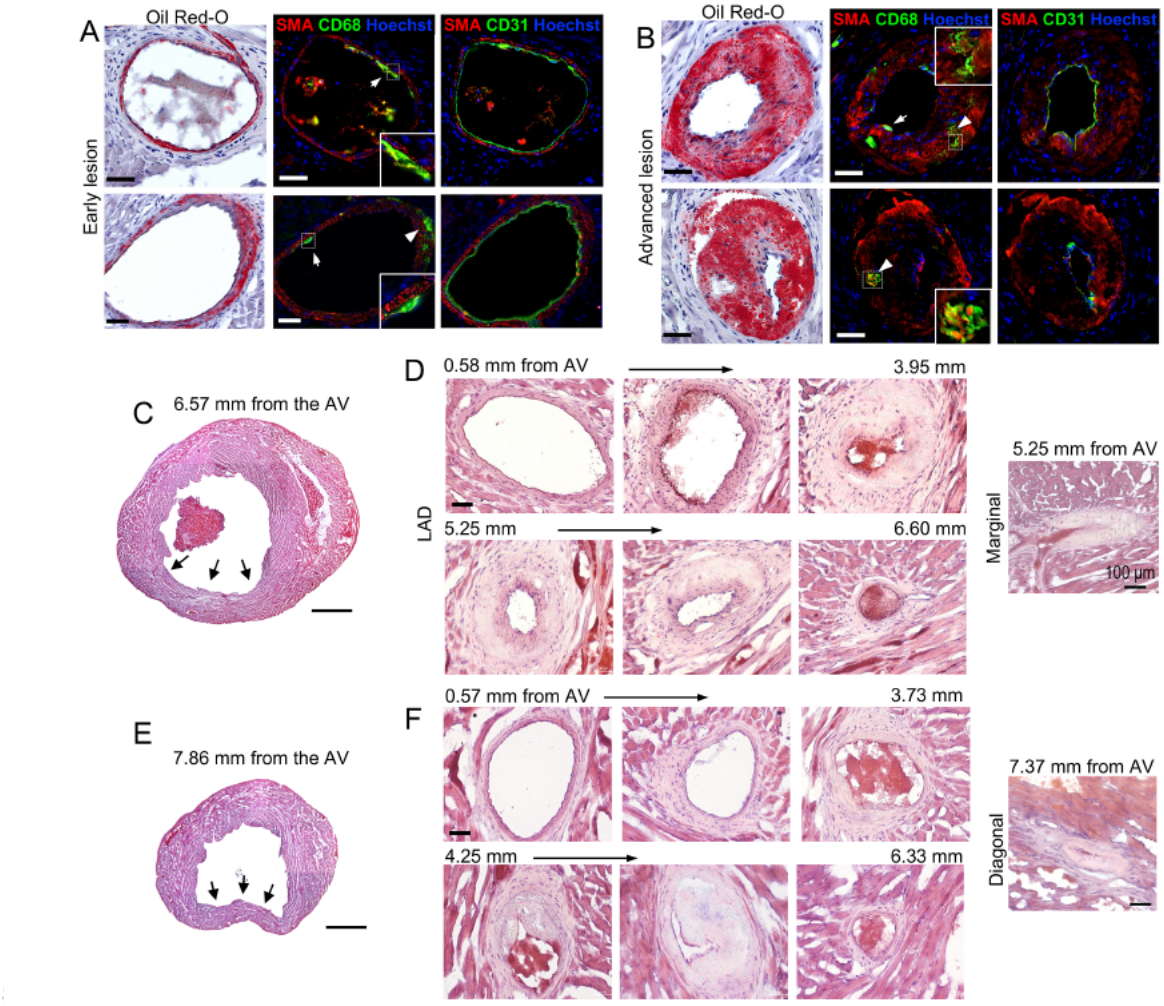

Supplemental Figure 7. Characterization of coronary lesions in Ldlr$^{-/-}$ mice at 15 weeks post-TAC. Sequential myocardial sections of Ldlr$^{-/-}$ mice died during physical stress protocol were stained with oil red-O & hematoxylin, and immunofluorescently stained with α-SMA (SMC, red), CD68 (monocyte/macrophage, green), CD31 (endothelial cells, EC, green) and Hoechst (nuclei, blue). (A) Oil red-O evidenced lipid accumulation in the vascular wall of early and (B) advanced coronary lesions. Consecutive heart sections immunofluorescently labeled showed macrophage (green) infiltration into the intima (white arrows) and media (white arrowheads) of the coronary arteries. Scale bars: 50 μm. (C-F) Myocardial sections from two Ldlr-/- mice died during the physical stress protocol. (C, E) Whole hearts sections at the indicated distance from the AV showed chronic myocardial infarctions, evidenced by the thinning of left ventricular wall (black arrows). Scale bars: 1 mm. (D, F) LAD of the corresponding hearts showing marked occlusions at different distance from the AV. (D) Marginal artery and (F) diagonal artery, in each heart, displayed an advanced degree of stenosis. Scale bars: 50 μm.